The c-Jun Amino-Terminal Kinase Pathway Is Preferentially Activated by Interleukin-1 and Controls Apoptosis in Differentiating Pancreatic β-Cells

Astrid Ammendrup, Anne Maillard, Karin Nielsen, Nina Aabenhus Andersen, Palle Serup, Ole Dragsbæk Madsen, Thomas Mandrup-Poulsen, and Christophe Bonny

To characterize the differentiation events that selectively target insulin-producing cells to interleukin (IL)-1β–induced apoptosis, we studied IL-1β signaling via mitogen-activated protein kinase (MAPK) and stress-activated protein kinase in 2 pancreatic endocrine cell lines. We studied the glucagon-secreting AN-glu cell line and the insulin and the islet amyloid polypeptide-producing β-cell line (AN-ins cells), which is derived by stable transfection of AN-glu cells with the transcription factor pancreatic duodenal homeobox factor-1. AN-ins cells were more sensitive to the cytotoxic action of IL-1β. This increased sensitivity was not associated with a more pronounced IL-1–induced nitric oxide production in AN-ins cells, but it correlated with a more marked activation of the 3 MAPKs extracellular signal–regulated kinases (ERKs)-1/2, c-Jun NH_2-terminal kinase (JNK), and p38 MAPK (p38). This led to increased phosphorylation of the transcription factors c-Jun, Elk-1, and ATF2 and of heat shock protein 25. Inhibition of ERK-1/2 and p38 did not prevent but aggravated IL-1β–induced cell death. In contrast, inhibition of JNK by transfection with the dominant negative inhibitor of the JNK-binding domain prevented apoptosis in both cell types. Cell death could be elicited by overexpressing the catalytic domain of MAPK kinase kinase 1, a specific activator of JNK and nuclear factor-κB, which does not recruit ERK-1/2 or p38. Coactivation of ERK-1/2 with JNK did not prevent apoptosis. In conclusion, increased MAPK signaling in response to IL-1β may represent a novel molecular marker of β-cell differentiation. JNK inhibition represents an effective means of preventing IL-1β–activated β-cell destruction. *Diabetes* 49:1468–1476, 2000

The β-cell mass is critical for glucose homeostasis and is dynamically regulated (1,2) with efficient apoptotic mechanisms to downsize the cell population when needed. This phenomenon is exemplified by the involution of the rat β-cell mass by apoptosis to adjust to the lesser need for insulin postpartum (3). Similarly, 50% of the endogenous β-cell mass disappears by apoptosis after implantation of a subcutaneous insulinoma in the rat (4). The apoptotic program appears linked to glucose metabolism and may be the ultimate guarantee for brain function to avoid fatal hypoglycemia (4). This innate vulnerability toward destruction may reflect the existence of constitutively active apoptotic programs in β-cells, which require glucose-induced protein synthesis to be repressed (5). Such active repression may fail or may be compromised during exposure to β-cell toxins, such as streptozotocin and cytokines (6), which have been implicated in the pathogenesis of type 1 diabetes (7–9).

The cytokines interleukin (IL)-1β in combination with tumor necrosis factor-α and interferon-γ cause apoptosis of rat and human pancreatic β-cells (7–9) and induce expression of the nitric oxide (NO)-synthesizing enzyme cytokine inducible NO synthase (iNOS), which results in intracellular NO synthesis in β- but not in α-cells (8).

Although NO may be one important mediator of cytokine-mediated rat β-cell destruction, NO alone does not seem to be sufficient to bring about this destruction. Blocking iNOS does not fully protect β-cells from cytokine-induced inhibition of insulin release (10), and NO synthesis and β-cell death are dissociated phenomena in human islets (8), suggesting alternative intracellular effector pathways induced by IL-1β and other cytokines.

Susceptibility to cytokine-mediated cytotoxicity appears to be dependent on the stage of β-cell differentiation (11). Thus, insulin-secreting phenotypes derived from pluripotent NHI and AN pancreatic endocrine cell lines were found to be more susceptible to IL-1β–induced cytotoxicity than the glucagon-secreting counterparts (11). Interestingly, NO release was found to be identical for NHI insulin and glucagon-secreting

From the Steno Diabetes Center and Hagedorn Research Institute (A.A., K.N., N.A.A., P.S., O.D.M., T.M.-P.), Gentofte, Denmark; and the Division of Medical Genetics (A.M., C.B.), Lausanne, Switzerland.

Address correspondence and reprint requests to Thomas Mandrup-Poulsen, MD, PhD, Steno Diabetes Center, 2 Niels Steensens Vej, DK-2820 Gentofte, Denmark. E-mail: tmpo@novo.dk.

Received for publication 3 April 2000 and accepted in revised form 26 May 2000.

N.A.A., P.S., O.D.M., and T.M-P. are employed by Novo Nordisk. P.S. and O.D.M. hold stock in Novo Nordisk, and P.S. and T.M.-P. have received funding from Novo Nordisk.

DMSO, dimethyl sulfoxide; DTT, dithiothreitol; ERK, extracellular signal–regulated kinase; FCS, fetal calf serum; GFP, green fluorescent protein; GST, gluthathione S-transferase; HSP, heat shock protein; IL, interleukin; iNOS, inducible NO synthase; JBD, JNK-binding domain; JNK, c-Jun NH_2-terminal kinase; LDH, lactate dehydrogenase; MAPK, mitogen-activated protein kinase; MAPKAP-K2, MAPK-activated protein kinase-2; MEK-1/2i, MAPK/ERK kinase-1 and -2 inhibitor; MKK, mitogen-activated protein kinase kinase; MTT, 3-(4,5-dimethylthiazol-2-yl)2,5-diphenyltetrazolium bromide; NF, nuclear factor; NO, nitric oxide; p38i, p38 inhibitor; MAPKi, MAPK inhibitor; PDX-1, pancreatic duodenal homeobox factor 1; PI, propidium iodide; SAPK, stress-activated protein kinase.

sublines (11). These findings support existence of differentiation-dependent proapoptotic pathways for IL-1β toxicity.

Recent studies have pointed toward the mitogen-activated protein kinases (MAPK) and the stress-activated protein kinase (SAPK) as signals for IL-1β toxicity to β-cells. Thus, IL-1β activated the c-Jun NH_2-terminal kinase (JNK) and the p38 kinase, as well as the extracellular signal–regulated kinases (ERKs)-1/2 in pancreatic β-cells (12). Combined inhibition of p38 and ERK-1/2 blocked NO synthesis, but inhibition of p38 partially prevented IL-1β–induced inhibition of insulin release independently of NO synthesis. Therefore, we reasoned that preferential MAPK/SAPK activation in the insulin-secreting subline might explain the differentiation-related and the acquired enhanced susceptibility to cytokine toxicity of these cells. Here we report that IL-1β caused a more marked activation of the ERK-1/2, the JNK, and the p38 kinases in insulin- versus glucagon-secreting AN cells. This translated into an increased phosphorylation of c-Jun, Elk-1, ATF2, and heat shock protein (HSP)-25, and it was associated with a higher sensitivity to IL-1β–induced toxicity. Inhibitors of p38 (p38i) and ERK-1/2 (MEKi) failed to prevent IL-1β–induced cytotoxicity and cell death. However, inhibition of JNK prevented IL-1β–induced apoptosis.

RESEARCH DESIGN AND METHODS

Media. RPMI-1640 glutamax, heat-inactivated fetal calf serum (FCS), penicillin/streptomycin, Hank's balanced salt solution without Ca^{2+} and Mg^{2+}, and trypsin were all from GibcoBRL (Paisley, Scotland, U.K.).

Reagents. All reagents were from Sigma (St. Louis, MO), unless otherwise specified. Authentic recombinant human IL-1β (1,400 U/ng) was from Novo Nordisk (Bagsværd, Denmark). Reagents for SDS-PAGE and the protein assay were all from Bio-Rad (Richmond, CA). [γ-^{32}P]ATP (3,000 Ci/mmol) and rainbow-labeled marker (high range) were from Amersham International (Buckinghamshire, U.K.). Gluthathione S-transferase (GST)–Elk-1 was a gift from Peter Shaw (Max-Planck-Institute für Immunobiologie, Freiburg, Germany), GST-ATF2 (1–109) was a gift from Roger J. Davis (Howard Hughes Medical Institute, University of Massachusetts Medical School). GST-Jun (1–89) was purchased from Stratagene Europe (Amsterdam, the Netherlands), and recombinant murine 25-kDa HSP-25 was purchased from Stressgen (Victoria, BC, Canada). Nitrocellulose membranes were from Schleicher & Schuell (Dassel, Germany), and total ERK-1/2 antibodies were acquired from New England Biolabs (Herfordshire, U.K.). MAPK-activated protein kinase-2 (MAPKAP-K2) antibody was from Upstate Biotechnology (Lake Placid, NY), horseradish peroxidase-conjugated goat anti–rabbit/–mouse IgG was from Bio-Rad, Tween 20 was from Merck (Darmstadt, Germany), and skimmed milk powder was from Milco (Copenhagen).

Inhibitors. The selective inhibitor of p38 MAPK (p38 MAPKi), SB203580 (13,14) (Compound VK-19.577; Vertex Pharmaceuticals, Cambridge, MA), completely blocks p38 MAPK activity in 10-μmol/l concentrations (13,14). Even at 100 μmol/l, this compound has no effect on a number of other kinases, including ERK-1/2 (14), although at 10 μmol/l, the JNK2β1 and JNK2β2 isoforms are inhibited by 75% (15). Compound PD 098059 from New England Biolabs is a specific inhibitor of MAPK/ERK kinase 1 and 2 (MEK-1/2i)(16–18), the upstream activators of ERK-1/2. MEK-1/2i fully inhibits ERK-1/2 activation at 100 μmol/l (10,11) without inhibition of JNK, p38 MAPK, and a wide range of other kinases investigated (16–18). p38MAPKi and MEK-1/2i were both dissolved in dimethyl sulfoxide (DMSO) to stock concentrations of 25 mmol/l and 10 mmol/l, respectively.

Cells and cultures. A mainly glucagon-expressing subline AN-glu, originally AN 1.2.9 (19), was derived from the pancreatic duodenal homeobox factor 1 (PDX-1)–negative pancreatic endocrine cell line (AN-697). When transfected with the transcription factor PDX-1, also known as STF-1 or IPF-1, this cell line expressed the (pro)insulin gene and was then termed AN-ins, originally AN 1.1.10. PDX-1 is a member of the homeodomain protein family, which plays a crucial role in both pancreatic development and insulin gene transcription (20). We chose these cell-lines because PDX-1 is critical for final β-cell maturation (21,22).

AN cells of low passage numbers (6–25) were cultured in 80-cm^2 tissue culture flasks (NUNC, Roskilde, Denmark) at 37°C in 5% CO_2 with a medium consisting of RPMI-1640 glutamax supplemented with 10% FCS, 1% penicillin/streptomycin, and 10% conditioned medium from NHI-ins phenotype cultures.

The insulin-secreting cell line βTC-3 (23) was cultured in RPMI-1640 medium supplemented with 10% FCS, 100 μg/ml streptomycin, 100 U/ml penicillin, and 2 mmol/l glutamine. INS-1 cells were cultured in the same medium supplemented with 50 mmol/l β-mercaptoethanol (24).

Viability assays. To investigate the effects of IL-1β alone or in combination with MAPK inhibitors on cell viability, we used the propidium iodide (PI) fluorescence assay from Sigma (St. Louis, MO). PI dye binds to the DNA when the cell membranes are permeable (dead cells), resulting in a fluorescence, which can be read on a fluorescence plate reader at 530 nm as excitation wavelength and with an emission filter of 620 nm (25).

Samples of 25 μl PI dye (50 μg/ml) were added to each well (100 μl) and were incubated for 15 min, after which 10 μl of 9% Triton X-100 (Sigma) was added for 60 min to lyse the cells. As a second method for assessing viability, we used the 3-(4,5-dimethylthiazol-2-yl)2,5-diphenyltetrazolium bromide (MTT) assay, also referred to as the CellTiter 96 nonradioactive cell proliferation assay from Promega, which determines mitochondrial activity. A dye solution (15 μl) containing tetrazolium salt was added to the cells in each 100 μl well. Culture medium and viable cells will convert this salt to a dark-colored formazan product within 4 h of incubation at 37°C and 5% CO_2. The formazan product was then solubilized by 100 μl stop solution and, after 1 h, it was read on an enzyme-linked immunosorbent assay plate reader at a wavelength of 570 nm (26,27). The number of viable cells is calculated by subtracting the number of dead cells from the number of total cells. At first we used a serum-deprived medium to minimize the background, but the use of a normal medium and a serum-deprived medium yielded identical viability data and were therefore pooled in these experiments.

Plasmids. The JNK-binding domain (JBD) (amino acids 1–280 of IB1 [28,29]) and the FLAG-JBD–expressing vectors in the plasmid pBK (Stratagene, Amsterdam) have been described previously (28). The pEGFP-N1 vector encoding the green fluorescent protein (GFP) was from Clontech (Basel). This plasmid was modified by inserting a FLAG sequence (Kodak) in frame with the GFP into the *Nhe*I site of the polylinker. This FLAG sequence starts with an ATG embedded in a Kozak's consensus to allow for efficient translation of the FLAG-GST fusion protein (pEGFP-FLAG construct). The constitutively active kinase domains of MEKK1 and MEKK2, ΔMEKK1 (1171–1493), and ΔMEKK2 (302–619) were cloned into the expression vectors pCDNA3 (Invitrogen, Groningen, the Netherlands) (30,31). For the experiments using episomal vectors, the JBD was cloned into the *Nhe*I/*Xho*I sites of the vector pCEP4 (Invitrogen, Groningen, the Netherlands) (30,31).

Transfections and apoptosis assays. A total of 3×10^5 cells were transfected with plasmids in 3-cm dishes using DOTAP (Boehringer Mannheim) and following the manufacturer's instructions. For experiments involving GAL-Jun (amino acids 1–89), GAL-ATF2 (amino acids 1–96), and GAL-Elk-1 (amino acids 307–428) (all from Stratagene), 20 ng of each of these plasmids was transfected with 1 μg of the reporter plasmid pFR-Luc (containing 5 repeats of the GAL4 DNA-binding site [Stratagene]) and 0.5 μg ΔMEKK1 or ΔMEKK2 for 24 h. The luciferase activities were measured using the dual reporter system from Promega (Wallisellen, Switzerland). To measure the number of apoptotic cells, the pEGFP-FLAG vector (0.5 μg) was transfected with either ΔMEKK1 or ΔMEKK2 (1 μg each) to visualize transfected cells. Cells were observed after 48 h under an inverted fluorescence microscope (Axiovert 25; Zeiss, Jena, Germany). Apoptotic cells were discriminated from normal cells by the characteristic blebbing of the cytoplasm and were easily determined by the fluorescence emitted by the GFP. Cells were also incubated with Hoechst 33342 and PI for 7 min before visualization under the inverted fluorescent microscope. A minimum of 1,000 cells in duplicate was counted for each experiment. The percentage of necrotic cells was identical (<0.5%) in control and IL-1–treated INS-1, βTC-3, AN-ins cells, and AN-glu cells. In the calculation of the apoptotic rate, the number of necrotic cells is included in the total number of cells.

MAP kinase experiments. To investigate the effect of IL-1β on ERK-1/2, JNK 1, and p38 MAPK activity, 150,000 cells · $well^{-1}$ · 200 μl^{-1} medium were preincubated in triplicate in 96-well plates (Costar, Cambridge, U.K.) for 24 h before incubation with IL-1β (concentrations from 0–3,500 pg/ml) for 20 min. The IL-1β exposure period of 20 min was based on previous time-response studies in rat islets (12), in which IL-1β mediated a peak phosphorylation of ERK-1/2 and p38 after 20 min. Medium was removed and 30 μl lysis buffer (20 mmol/l Tris acetate, pH 7.0, 0.27 mol/l sucrose, 1 mmol/l EDTA, 1 mmol/l EGTA, 1 mmol/l Na_3VO_4, 50 mmol/l NaF, 1% Triton X100, 5 mmol/l Na-pyrophosphate, 10 mmol/l β-glycerophosphate, 1 mmol/l dithiothreitol [DTT], 1 mmol/l benzimidine, and 4μg/ml leupeptin) were added, and the cells were left on ice for 30 min. The lysates were either used directly for the phosphotransferase assay or PI or stored at –80°C.

For the whole-cell lysate phosphotransferase assay, we used 5 μl whole-cell lysate, 17 μl reaction buffer (2 μg GST–Elk-1, 2 μg GST-ATF2, 1 μg HSP-25, 25 mmol/l Tris-HCl, pH 7.5, 0.1 mmol/l EGTA, 0.1 mmol/l Na_3VO_4, 1 μmol/l cAMP-dependent protein kinase inhibitor peptide, and 10 mmol/l Mg-acetate)

and 3 µl ATP-mix (1 mmol/l ATP and 3 µCi [γ-^{32}P]ATP). The GST–Elk-1, GST-ATF2, and HSP-25 phosphotransferase assays were carried out in a final volume of 25 µl at 30°C for 30 min. Reactions were terminated by addition of 25 µl of SDS sample buffer (125 mmol/l Tris-HCl, pH 6.8, 4% SDS, 0.1 mol/l DTT, 10% glycerol, and 0.02% bromophenol blue) and boiling for 5 min. The samples were then subjected to SDS-PAGE, as described by Laemmli (32), using a 4% stacking gel and a 12% separating gel. After electrophoresis, the separating gel was washed for 15 min in a mixture of 40% acetate and 10% methanol. The gels were dried and the proteins were visualized by autoradiography and quantitated by PhosphorImager (Molecular Dynamics, Kent, U.K.) (12).

Immunoprecipitation. Whole-cell lysate (100 µl) from AN-cells that was diluted 1:4 in washing buffer (lysis buffer with 0.1% Triton X-100) was immunoprecipitated by incubation overnight with anti–MAPKAP-K2 or anti–ERK-1/2 antibodies and then with protein A-sepharose beads (Pharmacia Biotech, Uppsala, Sweden) for 3 h at 4°C (MAPKAP-K2 and ERK-1/2). The beads were washed 3 times in washing buffer and twice in kinase buffer (20 mmol/l HEPES, pH 7.5, 20 mmol/l β-glycerophosphate, 10 mmol/l $MgCl_2$, 1 mmol/l DTT, and 50 µmol/l Na_3VO_4). Kinase reactions were carried out for 30 min at 30°C in 30 µl kinase buffer containing 10 µCi [γ-^{32}P]ATP and 1 µg HSP-25 (MAPKAP-K2) or 5 µg GST–Elk-1 (ERK-1/2). Reactions were terminated with 30 µl SDS sample buffer, and the samples were analyzed as in the MAP kinase assay.

JNK pull-down assay. Cell extracts were prepared as previously described, and 100-µg extracts were incubated for 3 h at 4°C with 1 µg GST-Jun on 10 µl glutathione-agarose beads (Sigma). After 4 washes with lysis buffer (containing 0.1% TX-100), the beads were resuspended in the same buffer supplemented with 10 mmol/l MgCl2 and 5 µCi γ^{33}P-ATP. After incubation at 30°C for 30 min, extracts were processed as prevously described. In βTC-3 cells, we observed that maximal JNK activity occurred between 1 and 3 h of treatment with IL-1β (10 ng/ml). Therefore, we prepared extracts after 1, 3, and 6 h of IL-1β treatment.

NO synthesis. Cell NO production was measured as nitrite accumulated in media determined by Griess reaction (33). In brief, 100 µl medium was mixed with an equal amount of the Griess reagent (one part 0.1% naphtylethylene diamine dihydrochloride and one part 1% sulfanilamide in 5% H_3PO_4 [Merck, Darmstadt, Germany]) and incubated for 10 min at room temperature. The absorbance at 550 nm was measured in an immunoreader (Nippon InterMed K.K., Tokyo). Values below the detection limit were assigned a quantity of 1 µmol/l. Intra- and interassay coefficients of variation were between 4.6 and 16.3% (11).

Statistics. Results are presented as means ± SE or SD as indicated in the figure legends. Wilcoxon's matched-pair and Student's *t* test were used, and $P < 0.05$ was chosen as the level of significance.

RESULTS

IL-1β induces higher MAP kinase activity in AN-ins than that in AN-glu cells. To investigate if MAPK/SAPK were activated differently by IL-1β in the insulin- versus the glucagon-producing cell line, we assayed the phosphotransferase activities toward Elk-1, ATF2, and HSP-25 in whole-cell lysates of IL-1β–stimulated AN-ins and AN-glu cells. Detectable kinase activity toward all 3 substrates was present in control cells of both cell lines (Fig. 1).

In AN-ins cells, 50 pg/ml IL-1β induced Elk-1 phosphorylation, which peaked to an almost 3-fold increase over baseline at 2,500 pg/ml of IL-1β. In the AN-glu cell line, 50 pg/ml IL-1β induced lower phosphorylation of Elk-1 compared with the AN-ins cell line, peaking with a 1.5-fold increase over baseline at 2,500 pg/ml IL-1β.

The phosphorylation of the substrate ATF2 was more pronounced than that of Elk-1 in both cell lines. In AN-ins IL-1β induced activation starting at 50 pg/ml and rising to a 7-fold

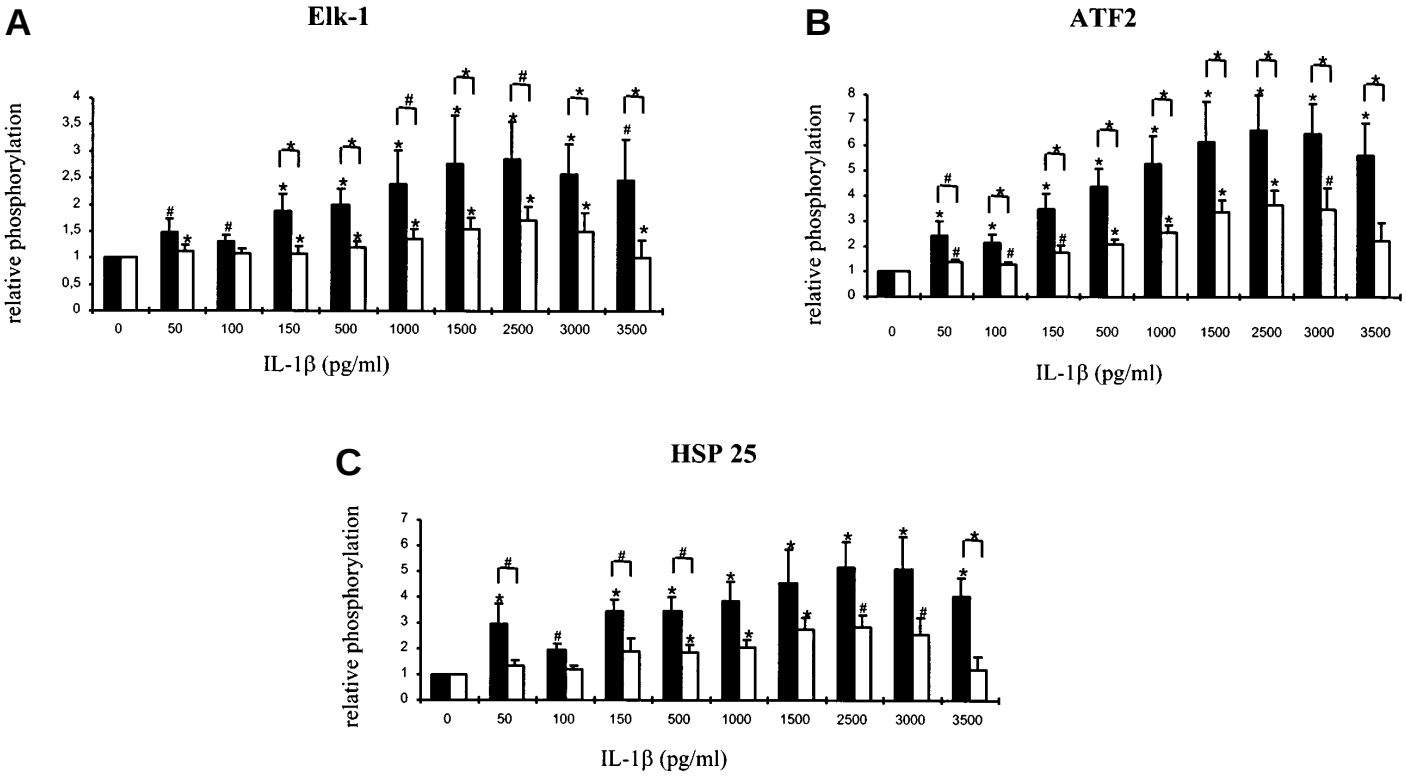

FIG. 1. IL-1β induces phosphotransferase activity in AN-ins and AN-glu. AN-ins (■) or AN-glu (□) cells were lysed after exposure to different concentrations of IL-1β for 20 min. Phosphorylation was quantified by PhosphorImager analysis and presented as means ± SE (*n* = 6) versus control cells treated without IL-1β (0). Elk-1 (*A*), ATF2 (*B*), and HSP25 phosphorylation (*C*). (Absolute values [counts per minute] for controls: Elk-1 AN-ins 70.0 ± 8, 0 × 10^4; Elk-1 AN-glu 61.1 ± 8, 7 × 10^4; ATF2 AN-ins 133.4 ± 24, 3 × 10^4; ATF2 AN-glu 135.4 ± 23, 6 × 10^4; HSP-25 AN-ins 45.0 ± 16, 4 × 10^4; HSP-25 AN-glu 54.4 ± 16, 6 × 10^4). Symbols above columns are significant differences versus respective controls; the brackets indicate significant differences between the cell lines. *$P < 0.02$; #$P < 0.05$.

increase in activation at 2,500 pg/ml. In the AN-glu cell line, IL-1β led to activation of ATF2 phosphorylation up to a 4-fold increase over baseline at 2,500 pg/ml.

In AN-ins cells, 50 pg/ml IL-1β induced significant HSP-25 phosphorylation, which peaked to a 5-fold increase over baseline at 2,500 pg/ml. In the AN-glu cell line, the phosphorylation of HSP-25 peaked at 2,500 pg/ml IL-1β with a 3-fold increase over baseline, showing no detectable activation below 500 pg/ml IL-1β.

ERK-1/2 and p38 inhibition decreases IL-1β–induced Elk-1 and HSP-25 phosphorylation but does not block ATF2 phosphorylation. To determine the role of ERK-1/2 and p38 in the IL-1β–induced Elk-1, ATF2, and HSP-25 phosphorylation, we incubated AN-ins cells with p38i and MEKi for 1 h before the addition of IL-1β. The MEKi (10 and 100 µmol/l) blocked the IL-1β–induced phosphorylation of Elk-1 but not of ATF2 and HSP-25 in the AN-ins cells (Fig. 2). The p38i at 10 µmol/l blocked HSP-25 phosphorylation, but it did not affect Elk-1 phosphorylation. When the 2 inhibitors were combined at 10 and 100 µmol/l concentrations, Elk-1 and HSP-25 phosphorylation was blocked, but ATF2 phosphorylation was unaffected, indicating that other kinases, such as JNK, are involved in ATF-2 phosphorylation in these cells.

IL-1β activates preferentially the ERK-1/2, p38, and JNK kinases in the AN-ins cells. To further determine the specificity of the kinase activity in the AN-ins and AN-glu cell lines, we measured kinase activity of ERK-1/2 and MAPKAP-K2, a downstream kinase of p38, by immunoprecipitation of whole-cell lysates.

Immunocomplexed ERK-1/2 phosphorylation of Elk-1 was more pronounced in AN-ins than AN-glu cells (Fig. 3*A*). ATF2 was not phosphorylated by ERK-1/2 in either cell line (data not shown), suggesting that ERK-1/2 is not involved in the ATF2 phosphorylation seen in the total lysate phosphotransferase assays. MAPKAP-K2 activity (Fig. 3*B*) was increased in the AN-ins cells compared with the AN-glu cells, peaking at 3,000 pg/ml IL-1β.

To measure JNK activity, we performed JNK pull-down assays. As shown in Fig. 3*C*, JNK was not significantly activated in the AN-glu cells after IL-1β treatment. However, JNK was markedly and significantly activated in the AN-ins cells (3-fold, $P < 0.01$). Taken together with the data obtained by the use of the ERK-1/2i and p38i, these data suggest that ERK-1/2, p38, and JNK are preferentially activated in the AN-ins subtype.

ERK-1/2 and p38 inhibition does not protect against IL-1β–induced cytotoxicity. The viability determined by PI of the 2 cell lines AN-ins and AN-glu were identical after 24 h of preincubation (AN-ins 3,789 ± 680 and AN-glu 4,000 ± 560 absorbance units, $n = 3$). First, we investigated whether IL-1β induced differential cytotoxicity in the AN-glu and AN-ins cell lines. We exposed the cells to IL-1β for 48 h before adding either PI or MTT. The AN-ins cell line was found to be 20–30% more sensitive to the toxic effect of IL-1β compared

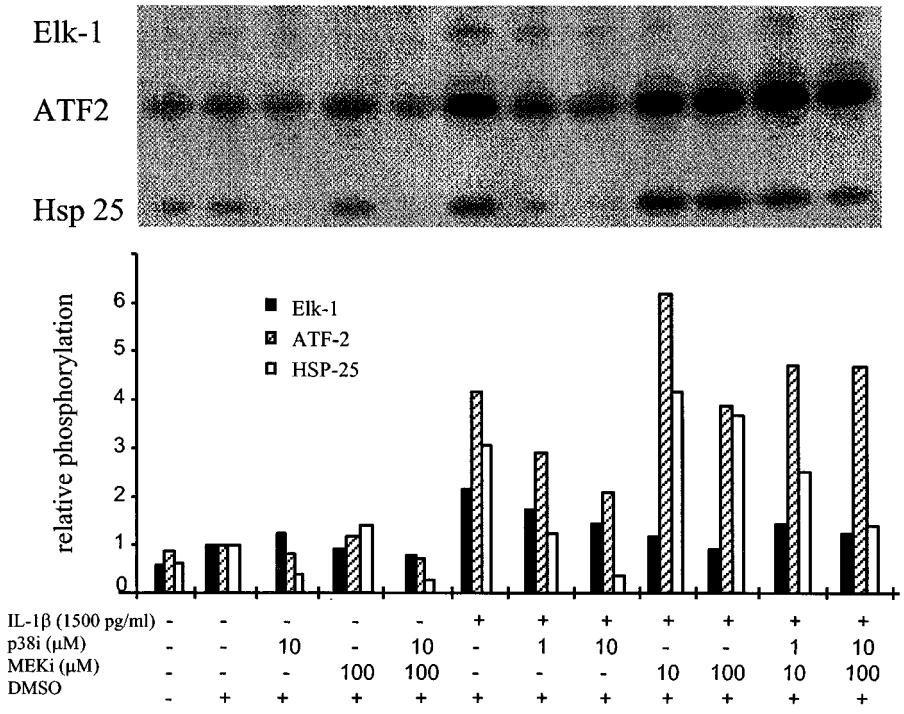

FIG. 2. ERK-1/2 and p38 inhibition inhibits IL-1β–induced Elk-1 and HSP-25 phosphorylation, but does not block ATF2 phosphorylation. Lysates were prepared from AN-ins cells that had been preincubated with MEKi and/or p38i 1 h before a 20-min exposure to 1.5 ng/ml of IL-1β. Whole-cell lysate kinase assay was performed with [γ-^{32}P]ATP and GST-Elk (Elk-1), GST-ATF2 (ATF2), and HSP-25 as substrates. Phosphorylation reactions were visualized after SDS-PAGE by autoradiography. Phosphorylation was quantified by PhosphorImager. A representative autoradiogram is shown (upper panel) with the quantified phosphorylations (lower panel). Data are presented as means ($n = 2$) versus control cells.

with the AN-glu cell line ($P < 0.002$ and 0.05 for MTT and PI, respectively, $n = 13$), confirming earlier findings using a lactate dehydrogenase (LDH) assay (11) (data not shown).

We next investigated if the difference in IL-1β–induced toxicity correlated with cellular NO production. Therefore, we measured medium nitrite release after 24 and 48 h in nonstimulated and IL-1β–exposed cells. After 24 h and 48 h, NO production did not differ between the AN-ins and AN-glu cell lines (data not shown).

We then sought to determine whether the MEKi and p38i prevented IL-1β–induced cytotoxicity to AN-ins cells. Using the PI assay, we noted a small but nonsignificant decrease in viability when the AN-ins cells were incubated with the inhibitors alone (Fig. 4*A*) or in combination (data not shown). The individual inhibitors potentiated rather than prevented IL-1β–induced cytotoxicity ($P < 0.05$; 5, 7.5, and 10 μmol/l VK, and 25, 50, 75, and 100 μmol/l PD) (Fig. 4*B*), and even more so in combination (data not shown). These data were reproduced using the MTT assay (data not shown)

JNK inhibition protects against IL-1β–induced apoptosis. To determine the role of the JNK pathway in regulating IL-1β–induced apoptosis, we transfected cells with vectors expressing the JBD of the JNK-interacting protein JIP-1 (28,29). In these experiments, cells were cotransfected with an expression vector encoding the GFP and control or JBD-expressing plasmids. After transfection, cells were incu-

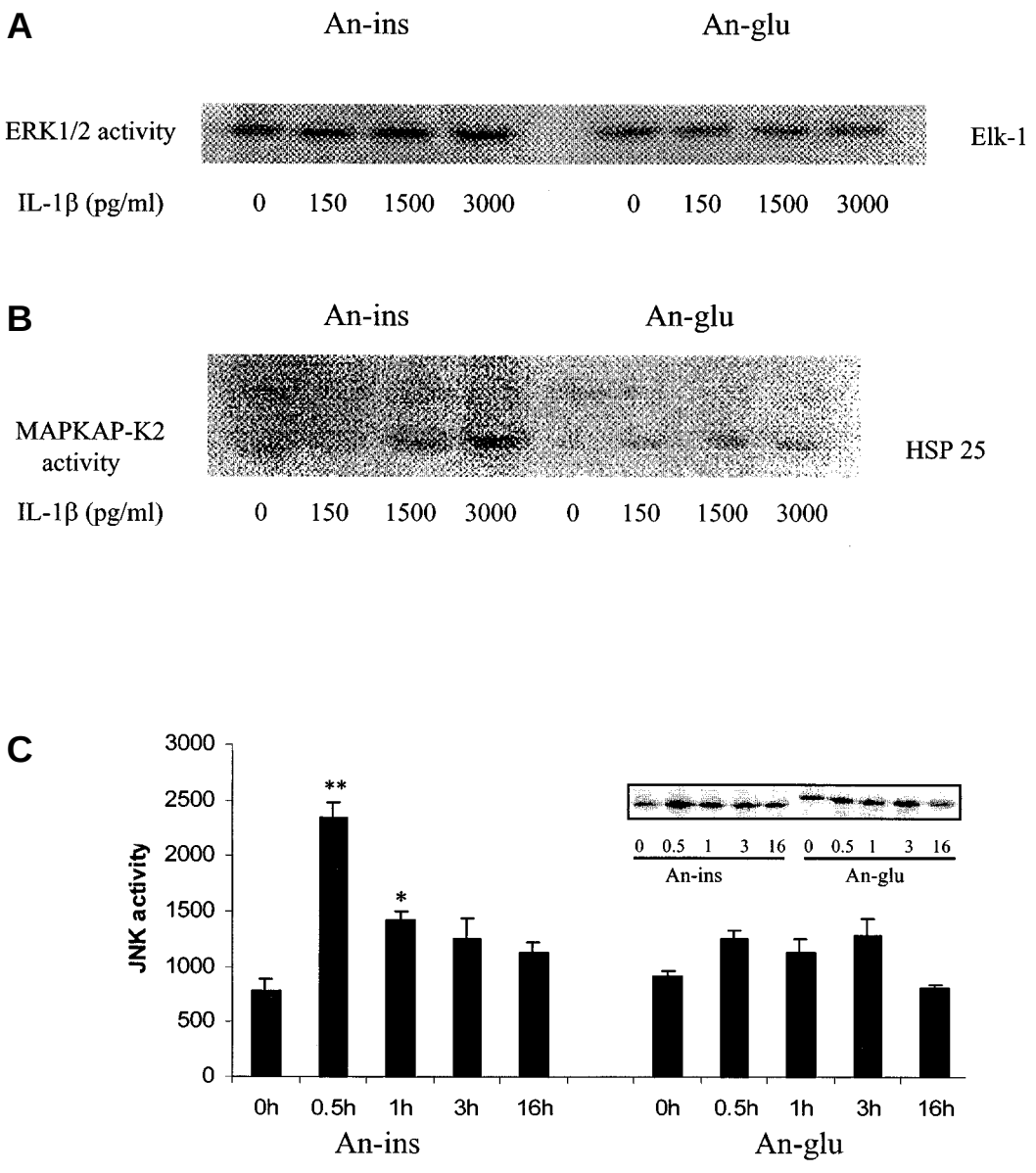

FIG. 3. ERK-1/2, JNK, and p38 kinase activity in AN cells. ERK-1/2 (panel A) and MAPKAP-K2 (panel B) were immunoprecipitated from lysates of IL-1β–exposed cells with specific antibodies, and their activity was measured in immunocomplex kinase assay with GST–Elk-1 (Elk-1) and HSP-25 as substrates, respectively. Phosphorylation reactions were initiated by the addition of [γ-^{32}P]ATP. After SDS-PAGE, phosphorylated proteins were visualized by autoradiography ($n = 2$). JNK (*C*) from lysates of cells that had been exposed to IL-1 (10 ng/ml) for 0–16 h was pulled down with GST-Jun (1–79). JNK activity was measured as the amount of GST-Jun phosphorylated following addition of [γ-^{32}P]ATP. After SDS-PAGE, phosphorylated proteins were visualized with an InstantImager apparatus (PerkinElmer). SDs are indicated; $n = 4$. *$P < 0.01$.

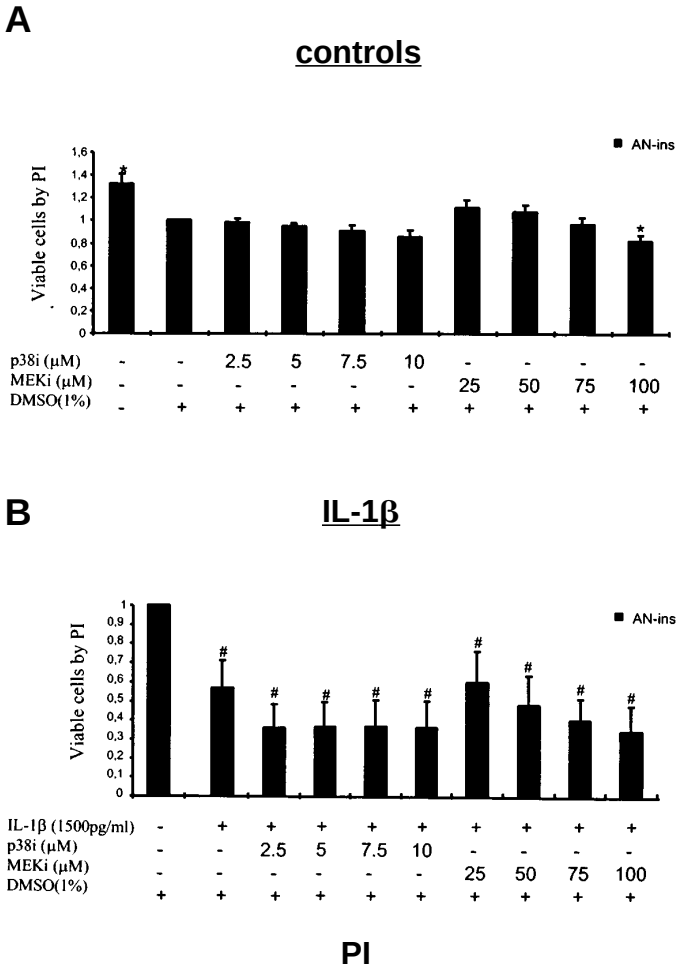

FIG. 4. ERK-1/2 and p38 inhibition does not protect against IL-1β–induced cytotoxicity. Cells were preincubated with MEKi and p38i 1 h before addition of IL-1β and were then incubated for 48 h before measuring viability. Effect of inhibitors alone (*A*) or in combination with IL-1β (*B*) on AN-ins cell viability, as measured by PI assay. Data are means ± SE (*n* = 6) versus control cells with DMSO. **P* < 0.02 vs. controls; #*P* < 0.05 vs. controls.

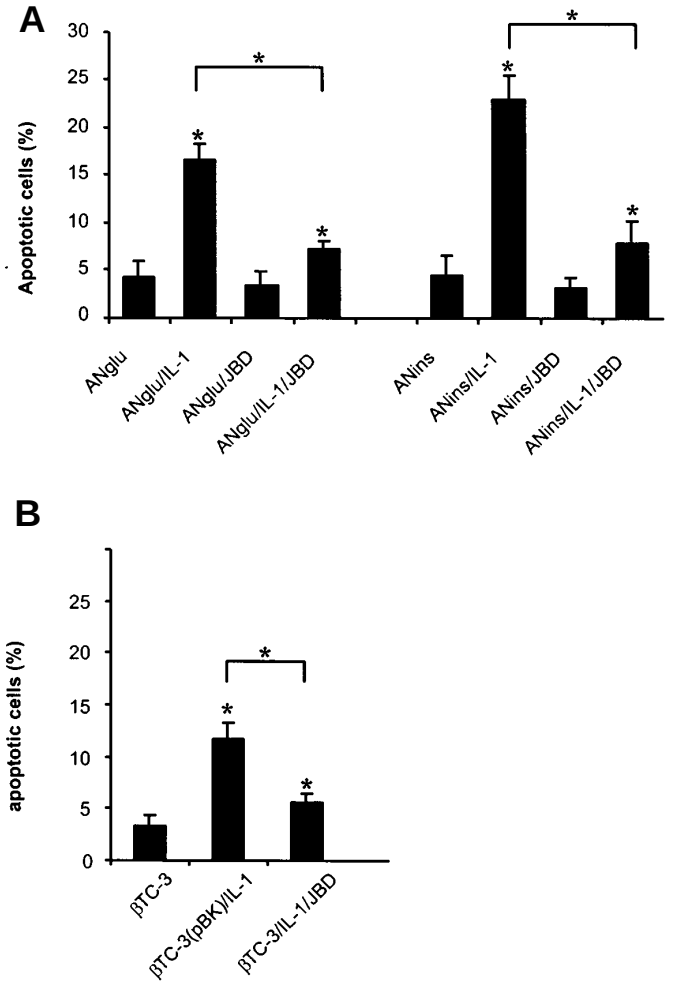

FIG. 5. JNK inhibition protects against IL-1β– and ΔMEKK1-induced apoptosis. AN-glu or AN-ins (*A*) were transfected with the indicated vectors and incubated with IL-1β (2.5 ng/ml) for 2 days. Apoptotic cells were then counted. βTC-3 cells (*B*) were either transfected with the indicated vectors for 2 days in the presence of IL-1β (10 ng/ml) or transfected for 24 h with the ΔMEKK1- and ΔMEKK2-expressing vectors. Apoptotic cells were then counted. Data are means ± SE (*n* = 4). **P* < 0.01 vs. controls.

bated with IL-1β for 2 days, and apoptotic cells were counted. In accordance with the data obtained using the MTT and PI assays, AN-ins cells were 35% more sensitive to the proapoptotic effect of IL-1 when compared with AN-glu cells. Overexpression of JBD reduced IL-1β–induced apoptosis by 80% (Fig. 5*A*). To establish that the protection conferred by JBD could be reproduced in other β-cell lines, we analyzed the mouse βTC-3 cell line in similar experiments. As shown in Fig. 5*B*, JBD potently protected this cell line from IL-1β–induced apoptosis. Similar results were also obtained with the rat INS-1 and RIN cell lines (data not shown).

We also performed transfection with episomal vectors bearing the hygromycine-resistance gene and expressing JBD. In the presence of IL-1β for up to 2 weeks, most cells died in control conditions, leaving about 10 hygromycine-resistant colonies. In cells stably expressing JBD, however, the number of hygromycine-resistant colonies was 2-fold higher with AN-glu cells and up to 35-fold higher with the AN-ins cells (Fig. 6*A*). Similar protection was also observed using βTC-3 cells (Fig. 6*B*). These data indicate that JBD not only protects cells against IL-1β–induced apoptosis, but also confers sufficient protection to allow a significant fraction of these cells to grow and divide in culture.

Preferential activation of JNK leads to apoptosis. We next tried to determine if preferential activation of JNK mimicked IL-1–induced apoptosis. JNK is mainly activated by the upstream kinases MEKK1, mitogen-activated protein kinase kinase (MKK)4, and MKK7. Overexpression of MKK4 or MKK7 did not induce β-cell apoptosis (data not shown). To achieve preferential activation of JNK, we therefore used the constitutively active form of the MAPK kinase kinase, ΔMEKK1. This mutant has little or no effect on ERK-1/2 and p38 activity, but it does induce nuclear factor (NF)-κB nuclear translocation (29,30). ΔMEKK1-mediated activation of c-jun, ATF2, and Elk-1, and these effects were prevented by JBD (Fig. 7*A*). ΔMEKK2, a strong and specific activator of ERK-1/2 did upregulate Elk-1 but not c-Jun or ATF2 activation (Fig. 7*B*). JBD had no effect on Elk-1 activated by ΔMEKK2.

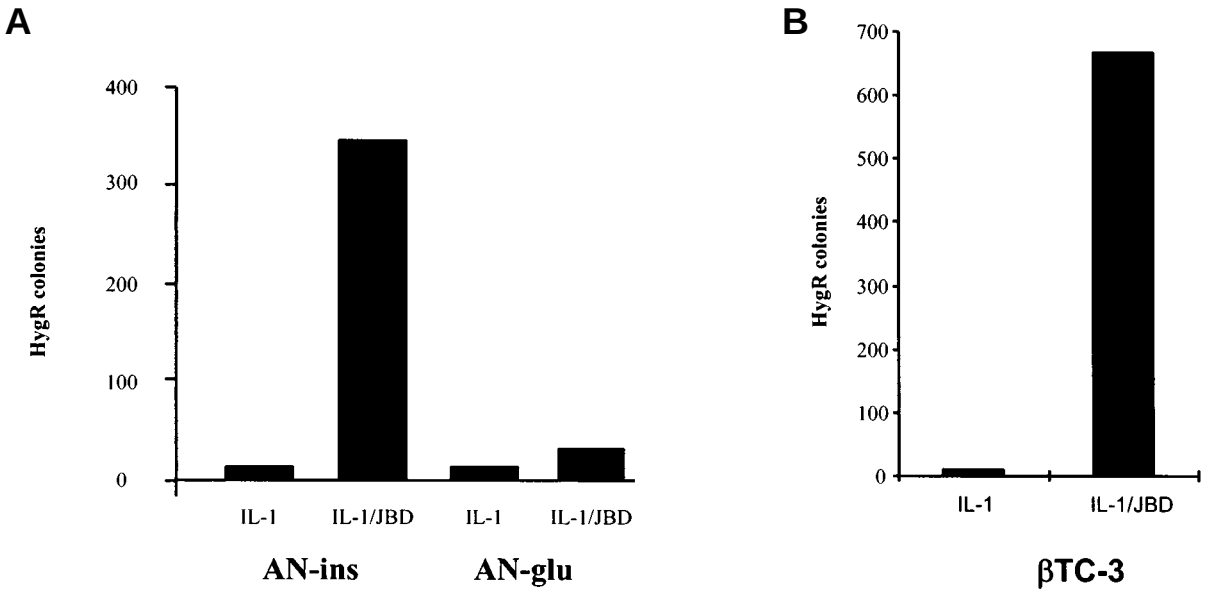

FIG. 6. JNK inhibition confers long-term protection against IL-1β–induced apoptosis. AN-glu or AN-ins (*A*) or βTC-3 (*B*) cells were transfected with the pCEP4 or pCEP4/JBD episomal vectors. After 2 days, transfected cells were selected with hygromycine (100 ng/ml) and IL-1β (2.5 ng/ml) was added. Cells were then incubated for 15 days in the presence of both hygromycine and IL-β, which were added to each change of medium (every 2–3 days). Colonies were then counted. Data are the means of 2 independent experiments.

As shown in Fig. 7*C*, ΔMEKK1 was a potent proapoptotic inducer in βTC-3 cells.

In an attempt to counterbalance this effect, we cotransfected cells with either JBD or with ΔMEKK2, because ERK-1/2 has been associated with protective effects on apoptosis in a number of cell systems (31). JBD prevented apoptosis induced by transfection with ΔMEKK1 (Fig. 7*C*). However, ΔMEKK2 was unable to prevent ΔMEKK1-induced apoptosis in these conditions. To ensure that the protective effect of JBD on β-cell survival correlated with JBD-induced inhibition of JNK activity, we cotransfected a reporter luciferase vector with a GAL–ATF-2–expressing construct and measured the transcriptional activity in presence of IL-1β and JBD. As shown in Fig. 8, JBD significantly prevented IL-1–induced activation of the GAL–ATF-2 construct.

DISCUSSION

This study demonstrates that transfection of a pancreatic endocrine glucagon-producing cell line with the transcription factor PDX-1 causing β-cell differentiation (19) led to a higher IL-1β–induced phosphorylation of the MAPK substrates Elk-1, ATF2, and HSP-25. We showed that ERK-1/2, as well as p38 and JNK, are constitutively activated in both AN-glu and AN-ins cells, and that the glucagon-producing cell line responded only weakly to IL-1β in terms of MAPK/SAPK activation. In contrast, IL-1β induced a more marked increase in MAPK/SAPK activities in the AN-ins cells.

The higher MAPK/SAPK activities in the insulin- versus the glucagon-producing cell line correlated with increased susceptibility of the AN-ins cells to IL-1β toxicity, as measured by both the MTT and PI assays. This difference in susceptibility to IL-1β–induced cytotoxicity between AN-ins and AN-glu has also been found using LDH release as a measurement of cell toxicity (11). The difference in toxicity was not associated with an increased induction of NO production in the AN-ins cells.

To investigate the possible causal relation between the higher IL-1β–induced MAPK/SAPK activation and susceptibility to IL-1β toxicity in the AN-ins than in the AN-glu cells, inhibitors of MEK-1/2, p38, and JNK were investigated for their possible protective effect of IL-1β–induced toxicity. The MEK-1/2 and p38 inhibitors themselves individually or in combination decreased viability of the AN-ins cells and augmented rather than protected against IL-1β–induced toxicity. This finding confirms recent studies in which the same inhibitors induced apoptosis in HIT-T15 cells and, when combined with IL-1β, potentiated rather than prevented apoptosis (34). In contrast, the blocking of JNK signaling by JBD prevented both IL-1β– and ΔMEKK1-induced apoptosis (Figs. 5 and 7*C*) and increased viability in control conditions (data not shown). The latter effect may reflect the high basal JNK activity observed in AN-ins cells.

Even if JNK appears necessary for the apoptotic response of all cell lines tested in this study, our data indicate that non-MAPK–signaling events contribute to the apoptotic response. Indeed, JBD conferred strong transient and weak long-term protection against cell death to AN-glu cells (Figs. 5 and 6). These protective effects were present even in the absence of an IL-1β–induced increase in JNK activity (Fig. 3*C*), and they indicate that the high basal levels of JNK activity are sufficient for apoptosis, providing that other signaling pathways are activated (e.g., NF-κB activation). Therefore, activation of JNK is likely to be a necessary rather than a sufficient event for the apoptotic response to develop (35).

It is known that transfection of murine glucagon-producing cell lines with the transcription factor PDX-1 activates the insulin gene as well as the islet amyloid polypeptide gene (6,19). This differentiation event creating AN-ins cells was sufficient to

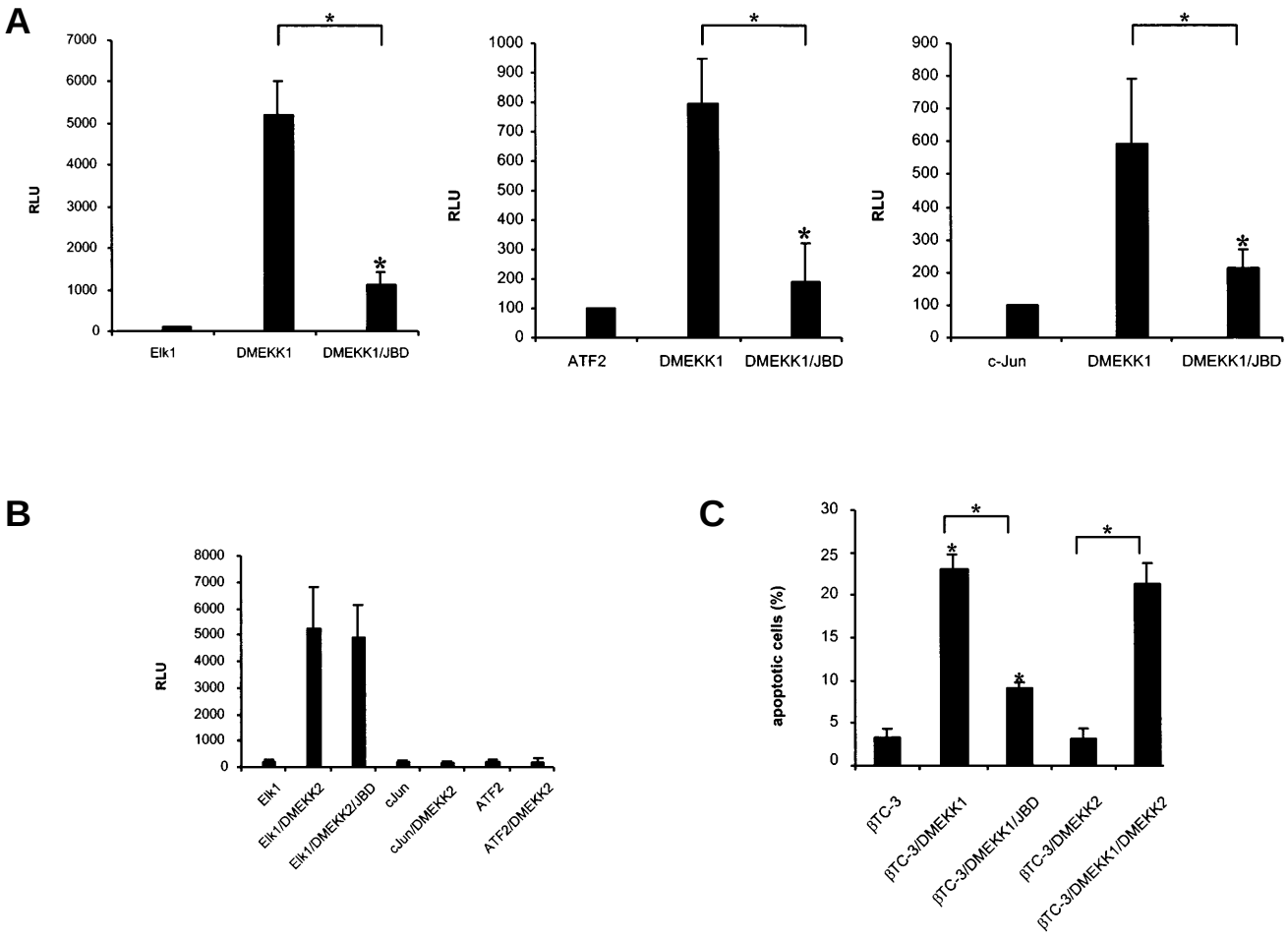

FIG. 7. Inhibition of JNK but not ERK-1/2–signaling by JBD, and JBD but not ΔMEKK2 overexpression prevents ΔMEKK1–induced apoptosis. βTC-3 cells were transfected with a 5 × GAL-LUC reporter plasmid with ΔMEKK1 (n = 8, *P < 0.01 vs. ΔMEKK1) (*A*), ΔMEKK2 (n = 4, *P < 0.01 vs. Elk-1) (*B*), JBD and GAL–Elk-1, GAL-ATF2, or GAL-Jun expression vectors as indicated. Empty vectors were added where necessary. Reporter LUC activities were measured 24 h later. βTC-3 cells were transfected with the indicated vectors as given in the legend to Fig. 6 (*C*). Apoptotic cells were counted after 24 h. Data are means ± SE (n = 4). *P < 0.01.

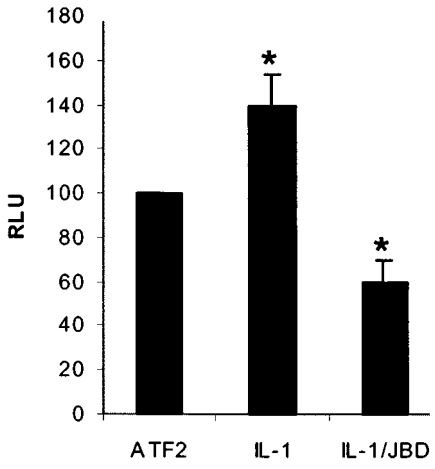

FIG. 8. JBD prevents IL-1–induced ATF2 activation. βTC-3 cells were cotransfected with a reporter luciferase vector and a GAL-ATF2–expressing construct or the relevant empty vectors. Cells were exposed to 10 ng/ml of IL-1β. Data are means ± SE (n = 5). *P < 0.05.

increase sensitivity to IL-1β and appears to be linked to an increased JNK signaling in these cells. Insulin is known to activate MAPK/SAPK in skeletal muscle (36), and it is possible that insulin cooperates with IL-1 on β-cells in this respect.

No significant differences in the expression of the IL-1 receptor–type 1 between the cell lines have been found (11), which negates the possibility that differences in IL-1β receptor number could account for the difference in IL-1β–induced MAPK activation and cytotoxicity. Thus, in addition to the known loss of scavenging potential to free radicals (37), this study has demonstrated that β-cells acquire enhanced signaling mechanisms via the MAPK/SAPK pathways during differentiation, and that PDX-1 targets β-cells to increased susceptibility to proapoptotic and toxic stimuli via the JNK pathway.

In conclusion, IL-1β induced a more marked phosphorylation of Elk-1, ATF2, c-jun, and HSP-25, as well as a higher ERK-1/2, JNK, and p38 activity in the AN-ins than in the AN-glu cell lines, which correlated with an increased susceptibility to IL-1β–induced cytotoxicity. Further, inhibition of JNK but not of p38 (p38i) and ERK-1/2 (MEK-1/2i) prevented IL-1β–induced apoptosis, demonstrating that JNK plays an important

proapoptotic role in these cell lines. The protective effects of JNK inhibition should be investigated further in primary cells, as well as in animal studies, to explore the role of JNK in the physiological regulation of β-cell mass and the possible therapeutic effects in type 1 diabetes.

ACKNOWLEDGMENTS

This study was supported by The Danish Research Council, The Danish Diabetes Association, Juvenile Diabetes Foundation International, Novo Nordisk, and the Swiss National Foundation for Scientific Research.

We thank Hanne Foght for excellent technical assistance, Dr. Christian Widmann for the generous gift of the MEKK expressing plasmids, and Lisbeth Brandt-Møller for secretarial help.

REFERENCES

1. Bonner-Weir S: Regulation of pancreatic β-cell mass in vivo. *Recent Prog Horm Res* 49:91–104, 1994
2. Finegood DT, Scaglia L, Bonner-Weir S: Dynamics of the β-cell mass in the growing rat pancreas. *Diabetes* 44:249–256, 1995
3. Scaglia L, Smith FE, Bonner-Weir S: Apoptosis contributes to the involution of β-cell mass in the postpartum rat pancreas. *Endocrinology* 136:5461–5468, 1995
4. Blume N, Skov J, Larsson L-I, Holst JJ, Madsen OD: Potent inhibitory effects of transplantable rat glucagonomas and insulinomas on the respective endogenous islet cells are associated with pancreatic apoptosis. *J Clin Invest* 96:2227–2235, 1995
5. Hoorens A, Van de Casteele M, Klöppel G, Pipeleers D: Glucose promotes survival of rat pancreatic β-cells by activating synthesis of proteins which suppress a constitutive apoptotic program. *J Clin Invest* 98:1568–1574, 1996
6. Watada H, Kajimoto Y, Miyagawa J, Hanafusa T, Hamaguchi K, Matsuoka T, Yamamoto K, Matsuzawa Y, Kawamori R, Yamasaki Y: PDX-1 induces insulin and glucokinase gene expression in αTC1 clone 6 cells in the presence of betacellulin. *Diabetes* 45:1826–1831, 1996
7. Mandrup-Poulsen T: The role of interleukin-1 in the pathogenesis of IDDM. *Diabetologia* 39:1005–1029, 1996
8. Eizirik DL, Flodström M, Karlsen AE, Welsh N: The harmony of the spheres: inducible nitric oxide synthase and related genes in pancreatic β-cells. *Diabetologia* 39:875–890, 1996
9. Corbett JA, Mikhael A, Shimizu J, Frederick K, Misko TP, McDaniel ML, Kanagawa O, Unanue ER: Nitric oxide production in islets from nonobese diabetic mice: aminoguanidine-sensitive and -resistant stages in the immunological diabetic process. *Proc Natl Acad Sci U S A* 90:8992–8995, 1990
10. Southern C, Schulster D, Green IC: Inhibition of insulin secretion by interleukin-1β and tumor necrosis factor-α via an L-arginine-dependent nitric oxide generating mechanism. *FEBS Lett* 276:42–44, 1990
11. Nielsen K, Karlsen AE, Deckert M, Madsen OD, Serup P, Mandrup-Poulsen T, Nerup J: β-cell maturation leads to in vitro sensitivity to cytotoxins. *Diabetes* 48:2324–2332, 1999
12. Larsen CM, Wadt KAW, Juhl LF, Andersen HU, Karlsen AE, Su MSS, Seedorf K, Shapiro L, Dinarello CA, Mandrup-Poulsen T: Interleukin-1β-induced rat pancreatic islet nitric oxide synthesis requires both the p38 and extracellular signal-regulated kinase 1/2 mitogen-activated protein kinases. *J Biol Chem* 273:15294–15300, 1998
13. Saklatvala J, Rawlinson L, Waller RJ, Sarsfield S, Lee JC, Morton FL, Barnes MJ, Farndale RW: Role for p38 mitogen-activated protein kinase in platelet aggregation caused by collagen or a thromboxane analogue. *J Biol Chem* 271:6586–6589, 1996
14. Cuenda A, Rouse J, Doza YN, Meier R, Cohen P, Gallagher TF, Young PR, Lee JC: SB 203580 is a specific inhibitor of a MAP kinase homologue which is stimulated by cellular stresses and interleukin-1. *FEBS Lett* 364:229–233, 1995
15. Whitmarsh AJ, Yang S-H, Su MS-S, Sharrocks AD, Davis RJ: Role of p38 and JNK mitogen-activated protein kinases in the activation of ternary complex factors. *Mol Cell Biol* 17:2360–2371, 1997
16. Dudley DT, Pang L, Decker T, Bridges A, Saltiel AR: A synthetic inhibitor of the mitogen-activated protein kinase cascade. *Proc Natl Acad Sci U S A* 92:7686–7689, 1995
17. Pang L, Sawada T, Decker SJ, Saltiel AR: Inhibition of MAP kinase kinase blocks the differentiation of PC-12 cells induced by nerve growth factor. *J Biol Chem* 270:3585–3588, 1995
18. Alessi DR, Cuenda A, Cohen P, Dudly DT, Saltiel AR: PD-098059 is a specific inhibitor of the activation of mitogen-activated protein-kinase kinase in vitro and in vivo. *J Biol Chem* 270:27489–27494, 1995
19. Serup P, Jensen J, Andersen FG, Jørgensen MC, Blume N, Holst JJ, Madsen OD: Induction of insulin and islet amyloid polypeptide production in pancreatic islet glucagonoma cells by insulin promoter factor 1. *Proc Natl Acad Sci U S A* 93:9015–9020, 1996
20. Madsen OD, Jensen J, Blume N, Petersen HV, Lund K, Karlsen C, Andersen FG, Jensen PB, Larsson L-I, Serup P: Pancreatic development and maturation of islet β-cells: studies of pluripotent islet cultures. *Eur J Biochem* 242:435–445, 1996
21. Ahlgren U, Jonsson J, Jonsson L, Simu K, Edlund H: β-cell-specific inactivation of the mouse Ipf1/Pdx1 gene results in loss of the β-cell phenotype and maturity onset diabetes. *Genes Dev* 12:1763–1768, 1998
22. Jensen J, Heller RS, Funder-Nielsen T, Pedersen EE, Lindsell C, Weinmaster G, Madsen OD, Serup P: Independent development of pancreatic α- and β-cells from neurogenin3-expression precursors: a role for the Notch pathway in repression of premature differentiation. *Diabetes* 49:163–176, 2000
23. Efrat S, Linde S, Kofod H, Spector D, Delannoy M, Grant S, Hanahan D, Baekkeskov S: β-cell lines derived from transgenic mice expressing a hybrid-insulin gene-oncogene. *Proc Natl Acad Sci U S A* 85:9037–9041, 1988
24. Asfari M, Janjic D, Meda P, Li G, Halban PA, Wollheim CB: Establishment of 2-mercaptoethanol-dependent differentiated insulin-secreting cell lines. *Endocrinology* 130:167–178, 1992
25. Dengler WA, Schulte J, Berger DP, Mertelsmann R, Fiebig HH: Development of a propidium iodide fluorescence assay for proliferation and cytotoxicity assays. *Anticancer Drugs* 6:522–532, 1995
26. Mosman T: Rapid colorimetric assay for cellular growth and survival: application to proliferation and cytotoxicity assay. *J Immunol Methods* 65:55–63, 1983
27. Campling BG, Pym J, Galbraith PR, Cole SPC: Use of the MTT assay for rapid determination of chemosensitivity of human leukemic blast cells. *Leuk Res* 12:823–831, 1988
28. Bonny C, Nicod P, Waeber G: IB1, a JIP-1-related nuclear protein present in insulin-secreting cells. *J Biol Chem* 273:1843–1846, 1998
29. Dickens M, Rogers JS, Cavanagh J, Raitano A, Xia Z, Halpern JR, Greenberg ME, Sawyers CL, Davis RJ: A cytoplasmic inhibitor of the JNK signal-transducting pathway. *Science* 277:693–696, 1997
30. Lee FS, Hagler J, Chen ZJ, Maniatis T: Activation of the 1κBα kinase complex by MEKK1, a kinase of the JNK pathway. *Cell* 88:213–222, 1997
31. Xia Z, Dickens M, Raingeaud, J, Davis RJ, Greenberg ME: Opposing effects of ERK and JNK-p38 MAP kinases on apoptosis. *Science* 270:1326–1331, 1995
32. Laemmli UK: Cleavage of structural proteins during the assembly of the head of bacteriophage T4. *Nature* 227:680–685, 1970
33. Green LC, Wagner DA, Glogowski J, Skipper PL, Wishnok JS, Tannenbaum SR: Analysis of nitrate, nitrite, and [^{15}N]nitrate in biological fluids. *Anal Biochem* 126:131–138, 1982
34. John NE, Belin VD, Harrison MJ, Andersen NA, Mandrup-Poulsen T, Green IC: Kinase inhibitor effects on spontaneous and cytokine-induced apoptosis in HIT-T15 cells and neonatal rat islets (Abstract). *Diabetologia* 41 (Suppl. 1):A161, 1998
35. Widmann C, Johnson NL, Gardner AM, Smith RJ, Johnson GL: Potentiation of apoptosis by low-dose stress stimuli in cells expressing activated MEK kinase 1. *Oncogene* 15:2439–2447, 1997
36. Moxham CM, Tabrizchi A, Davis RJ, Malbon CC: Jun N-terminal kinase mediates activation of skeletal muscle glycogen synthase by insulin in vivo. *J Biol Chem* 271:30765–30773, 1996
37. Hohmeier H-E, Thigpen A, Tran VV, Davis R, Newgard CB: Stable expression of manganese superoxide dismutase (MnSOD) in insulinoma cells prevents IL-1β-induced cytotoxicity and reduces nitric oxide production. *J Clin Invest* 101:1811–1820, 1998